Strategy for active mixing in microdevices

Boris Stoeber,[1,*] Dorian Liepmann,[2] and Susan J. Muller[3]
[1]*Department of Mechanical Engineering and Department of Electrical and Computer Engineering, University of British Columbia, Vancouver, British Columbia, Canada V6T 1Z4*
[2]*Department of Bioengineering, University of California, Berkeley, California 94720, USA*
[3]*Department of Chemical Engineering, University of California, Berkeley, California 94720, USA*
(Received 6 November 2006; revised manuscript received 24 April 2007; published 28 June 2007)

We present a concept for and experimental demonstration of an active microfluidic mixer that uses microvalves to control periodic flow deviation. This active design allows the degree of mixing to be varied independently of flow rate. The mixer is compact and efficient, achieving mixing of different fluids through chaotic advection by stretching and folding the interface of the fluids.

DOI: 10.1103/PhysRevE.75.066314 PACS number(s): 47.61.Ne, 47.51.+a, 47.61.Fg

Rapid mixing over short length scales in microfluidic devices is crucial for efficient control of reaction kinetics and for controlled manipulation of biological fluids in micro total analysis systems (MicroTAS). However, MicroTAS generally operate at very low flow velocities v and the corresponding low Reynolds numbers $\mathrm{Re}=Lv\rho/\eta\sim 10^{-2}$ (with L a typical length scale such as the channel width W, ρ the mass density, and η the shear viscosity of the fluid) indicate laminar flow so that mixing mainly occurs through molecular diffusion across streamlines [1]. Even though microfluidic channels are narrow ($W\sim 100\ \mu$m), mixing of costreaming fluids based purely on molecular diffusion is slow; the ratio of diffusion to convection times scales, given by the Péclet number $\mathrm{Pe}=vW/D>100$ (with D the molecular diffusivity), is high in these systems [1]. Faster mixing can be achieved by reducing the cross-layer diffusion length [2,3], and different strategies have been proposed to accomplish this by generating either well-ordered thin fluid layers or chaotic flow patterns [1,4] of the fluids to be mixed. The generation of large interfaces, achieved, for example, through stretching, is crucial for mixing [2].

Passive mixers, attractive because they do not involve active elements, either generate thin parallel layers of the fluids [1,5] or achieve chaotic flow patterns through channel design [6–8]. While effective passive micromixers have been developed, they require long mixing lengths and flow channels, cannot simply be turned off, and the degree of mixing cannot be adjusted independent of the flow rate. Various mixing methods based on *active* flow manipulation have also been developed. Some active micromixers cause bulk flow disturbances in a channel, where forces perpendicular to the undisturbed streamlines induce secondary flow patterns [9,10]; others rely on periodic cross-channel flow in and out of side channels [11] to disturb the fluid streamlines, often involving complex fabrication processes or dead volumes that are difficult to fill and require secondary pumping mechanisms. Two-phase systems have also been used for mixing [12]; these require phase separation after mixing.

Here we present a simple and effective mixing approach that uses two active valves to produce alternating periodic deviation of the flow into each of two parallel branches in a short section of the flow system [Fig. 1(a)]. Valving is achieved through the thermally triggered phase transition of a biocompatible solution of Pluronic polymers that is used as the working fluid of the microfluidic system [13]. Pluronic solutions gel at elevated temperatures, but are liquid at low temperatures. Activating a heater integrated in the wall of a microchannel results in localized gel formation of the working fluid leading to blockage of the channel to flow, thus

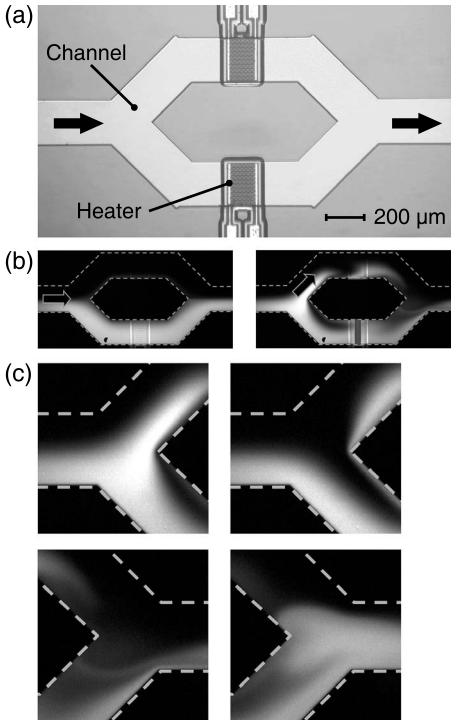

FIG. 1. Mixing of two fluids in an active two-stage micromixer. (a) Optical micrograph of the flow channel system. (b) Left: two fluids are streaming through the mixer, one of the fluids is fluorescently labeled; right: an instance in the mixing cycle during which the valve in the lower side channel is closed. (c) Top left and right: the first stage of the mixer, the channel bifurcation, during two instances in the mixing cycles; bottom left and right: the second mixing stage, the junction, where the streams from the two branches form alternating bulges spanning the width of the main channel.

*stoeber@mech.ubc.ca

acting as a closed valve [14]. Once heating is stopped the heat dissipates rapidly into the substrate leading to liquefaction of the gel, thus opening the valve. Any rapidly responding microvalves could be employed in our mixing strategy; here the Pluronic valves allow objective evaluation of the performance of the mixing concept because they do not add a significant flow disturbance on actuation.

Consider two parallel streams of different liquids A and B flowing in the upstream channel in Fig. 1(a) due to a pressure gradient. Through periodic diversion of both streams alternately into the upper and lower parallel branches of the mixer, mixing of the streams is promoted at two stages: the upstream bifurcation of the channel and the downstream junction. At the upstream bifurcation, diversion of both streams first into the upper branch and then into the lower branch results in alternating packets of fluid A and B along the inner half of each channel [see Fig. 1(b) and Ref. [15]]. As these packets of fluid travel though the parallel branches they undergo dispersion in the flow direction, while further smearing is caused by molecular diffusion across streamlines. At the second mixing stage (the junction), the flow from one branch ideally spans the entire width of the exit channel before switching to the other branch; from there the pressure-driven advective transport along the channel results in the plugs being stretched to very thin fluid layers.

The effectiveness of these two mixing stages can be related to the Strouhal number $\mathrm{Sr}=fL/v$ that depends on the frequency of one mixing cycle f, the average flow velocity v, and a characteristic length scale L for the respective mixing stage. This length scale corresponds to the optimum displacement of the fluid streams during one operation cycle leading to maximum flow disturbance. For two fluids at equal volumetric flow rates, the Sr dependence can be illustrated for two extreme cases; for very fast valve actuation ($\mathrm{Sr}\rightarrow\infty$) the two streams will stay separated in their two respective mixer branches, and no mixing will be achieved. At very slow valve actuation ($\mathrm{Sr}\rightarrow 0$), both streams will basically flow side by side through either branch.

At intermediate Sr, the first mixing stage [Fig. 1(c) top] will show optimum performance if the fluid is displaced by about one channel width W during one half mixing cycle $f\approx v/(2W)$. Lower frequencies will result in longer packets of fluid A in B (and vice versa) in the inner halves of the parallel branches, thus reducing the degree of mixing; higher frequencies will result in progressively smaller amounts of the lower fluid component reaching the upper channel (and vice versa). However, the second stage [Fig. 1(c) bottom] will show optimum performance if the fluid bulge exiting one mixer branch spans the entire width of the exit channel; based on the flow field this is achieved for a fluid displacement of around two channel widths during one half mixing cycle $f\approx v/(4W)$. The operating conditions of both mixing stages can be set independently at a given frequency by choosing appropriate channel widths at the bifurcation and at the junction. Thus, through channel design, the mixing performance can either be optimized for one specific Sr or made essentially invariant to Sr. The chosen mixer layout [Fig. 1(a)] allows mixing over a wide range of Sr.

Figure 1(b) (left) shows the case where two fluids are introduced into the main flow channel at equal flow rate. One

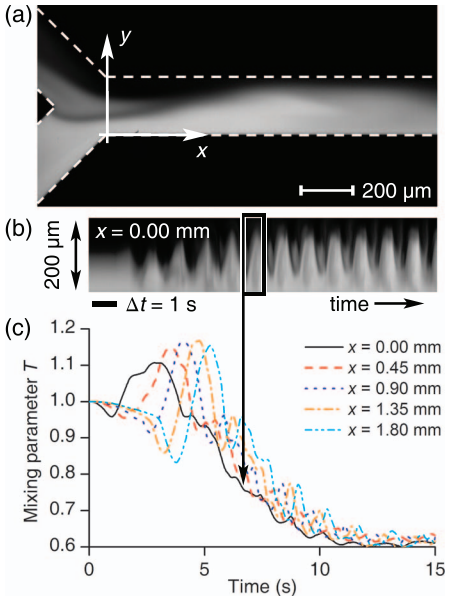

FIG. 2. (Color online) Characterization of the two-stage micromixer. (a) The location x in the exit channel is measured from the channel junction. (b) The fluorescence brightness of the fluid in the exit channel is recorded across the channel as a function of time. (c) Mixing parameter T as a function of time at five different locations x downstream from the channel junction.

of the two fluids was labeled with the fluorescent dye fluorescein. Figure 1(b) (right) shows the mixer during operation. The distribution of brightness levels of the fluid can serve as a measure for mixing performance in the exit channel shown in Fig. 2(a) and Ref. [15], assuming the fluorescence intensity of the fluid is proportional to the fluorescein concentration. We neglect concentration variations along the channel height since the time scale for diffusion across the flow channel $t_D\approx H^2/(16D)=0.37$ s, is of the same order as the convection time $t_C=L/v$, where L is the length of a liquid plug, for all experiments. Figure 2(b) shows the time evolution of fluorescence intensity across the exit channel (in the y direction) at the channel junction. The degree of mixing at any channel location x can be quantified by evaluating the pixel intensity $I=I(x,y,t)$ across the channel at that location x over one period of mixer operation. Normalizing the standard variation of these intensity values (along y and t) by the average intensity yields a measure of mixing

$$S=\left[\overline{(I/\bar{I}-1)^2}\right]^{1/2},$$

where a bar over a quantity denotes the arithmetic mean over one period. This quantity is normalized by its value before mixer operation S_0 (which corresponds to the limit $\mathrm{Sr}\rightarrow\infty$) to achieve an objective measure for mixing performance $T=S/S_0$ that is independent of any diffusive mixing that occurs without mixer operation. Values of this mixing parameter T close to 1 indicate poor mixing, while values close to 0 correspond to completely mixed fluids with a spatially uniform fluorescence intensity [6–9,11,12].

Figure 2(c) shows T as a function of time for five locations downstream of the junction in Fig. 2(a). The initial high

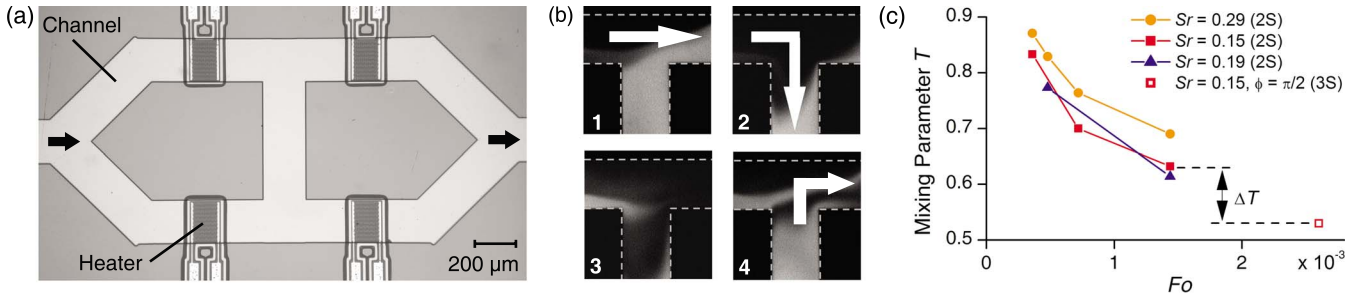

FIG. 3. (Color online) (a) Optical micrograph of the three-stage mixer with four heater-valves and the center channel connecting both parallel branches. (b) Fluorescence intensity of the fluids at the third stage of the three-stage micromixer during the four steps of the mixing cycle. (c) Mixing parameter T as a function of Fo for different Sr of the two-stage mixer (2S) and for the three-stage mixer (3S); ΔT: improved performance of the three-stage mixer over the two-stage mixer at identical throughput Q.

fluctuations in T correspond to highly skewed bimodal brightness distributions during the first mixing cycles, where only the second mixing stage at the channel junction contributes to a disturbance of the initially purely parallel streams. The mixing parameter T reaches its steady-state value later at locations further downstream in the flow channel. This delay corresponds well with the fluid convection time between the different locations of observation. The steady-state value of T is similar for all locations, indicating that dispersion is not effective over the short distances considered, and the measured mixing is mainly achieved through flow deviation in the mixer. This also confirms the assumption of uniform brightness distribution across the channel depth.

Mixing in the two-stage mixer was quantified for Sr=0.07 to 1.16. Significant mixing enhancement was achieved over a wide range of Sr with a minimum value for the mixing parameter $T=0.61$ at Sr=0.19. The two-stage mixer shows a high performance for a mixer length of only 1.1 mm, thus taking up very little real estate on a MicroTAS chip. Reducing the characteristic length scales of the mixing stages and optimizing mixer operation would lead to an improved spatial distribution of the two fluids and hence to better mixing, however, this would have been difficult to evaluate experimentally due to the physical resolution limits. Further improvement of the mixing performance for the present devices could be achieved by arranging several two-stage mixers in series. Alternatively, a third mixing stage can be introduced to form a three-stage mixer [Fig. 3(a)].

The three-stage mixer has two additional valves, one located in either branch; a central channel connects the parallel branches between their two valves [Fig. 3(a)]. The additional mixing stage consists of the T-shaped channel section in both the upper and the lower branches of the mixer. Through appropriate cycling of the four valves, fluid from one branch can move from the T junction into the center channel and then back out as it moves downstream [see Fig. 3(b) and Ref. [15]]. During this flow deviation, the fluid layers undergo chaotic stretching and folding, leading to thinner fluid layers with a longer interface.

The two first valves in either branch must be operated out of phase to guarantee continuous flow through the mixer, and each valve should be opened and closed the same amount of time for optimum mixer performance. The second pair of parallel valves will be driven in the same manner, at the same frequency f, while the phase difference φ between the operation cycles of both pairs is a new parameter that affects the flow pattern, residence time of fluid in the mixer, and the mixer performance. If both valve pairs are operated in phase ($\varphi=0$), the center channel is unused (fluid stays in this center channel without any exchange) and the three-stage mixer operates as a two-stage mixer. If both valve pairs are operated out of phase by $\varphi=\pi$, all fluid undergoes stretching and folding during flow into and out of the center channel. The additional residence time due to temporary storage of fluid in the center channel alone will lead to a slight mixing enhancement through molecular diffusion; this additional residence time depends on the value of φ, the volume of the center channel, and the mixer throughput Q, which can be chosen independently.

The residence time of the fluid in the mixer t_R can be normalized by the characteristic time scale for cross-channel diffusion $\tau=W^2/D$ to construct a Fourier number $\mathrm{Fo}=Dt_R/W^2$. Figure 3(c) shows the mixing parameter as a function of the Fourier number for different Sr for the two-stage mixer and for the three-stage mixer at Sr=0.15 and $\varphi=\pi/2$. The Reynolds number for all experiments was in the range $3.8\times10^{-4}<\mathrm{Re}<1.5\times10^{-3}$. Experiments with the same Fourier number allow the same amount of molecular diffusion within the fluids while passing through the mixer so differences in the mixing parameter T are due to the chaotic flow patterns achieved by the mixer. The mixing parameter for the two-stage mixer at fixed Fo shows a weak dependence on Sr [Fig. 3(c)], consistent with the layout of the flow channels that promotes mixing over a broad range of Strouhal numbers. Figure 3(c) also shows that the three-stage mixer provides better mixing (by ΔT) at the same throughput Q as the two-stage mixer even for the simple mode of operation chosen for this experiment ($\varphi=\pi/2$).

The concentration distribution of two parallel streams of equal flow rate in a channel [1] due to molecular diffusion can be approximated by $c(x,y)\sim\bar{c}+f(y/W)\exp[-\pi^2x/(\mathrm{Pe}W)]$, which leads to a mixing parameter $T=\sqrt{1/W\int f^2(y/W)dy}\exp[-\pi^2x/(\mathrm{Pe}W)]$. We apply this distribution to the case of a stretched and folded interface by replacing the linear streamwise coordinate x with a coordinate $\tilde{x}$ along the interface. Stretching the original interface Σ_0 to Σ_1 reduces the effective channel width to $W_1=W\Sigma_0/\Sigma_1$. This does not affect the value of the square

root in the expression for T, which is normalized with respect to the channel width. Scaling with time and location x occurs through the exponent, where the channel width W is a convective scaling for x and stays therefore unchanged. However, Pe scales with the effective channel width W_1 as it describes cross-channel diffusion. Thus, the mixing parameter $T=g(y/W)\exp(-\pi^2\,\mathrm{Fo}\,\Sigma_1/\Sigma_0)$ can also be expressed in terms of Fo. This is consistent with Fig. 3(c), where the value of T decays exponentially with Fo, and T depends on the Sr, which affects the stretching of the interface and hence the value of Σ_1/Σ_0. This Fo dependence of the mixing parameter is therefore an additional measure for the effectiveness of the mixer in stretching and folding of the fluid.

Finally, we can compare the performance of our compact mixer to that of Stroock *et al.* [8] for the mixer lengths $L_2=1.4$ mm and $L_3=2.2$ mm corresponding to the two- and three-stage mixers, respectively. For this purpose, values for the mixing parameter $T_L=\sigma(\Delta y=L)/\sigma(\Delta y=0)=2\sigma(\Delta y=L)$ were calculated from the data in Fig. 3(D) of Ref. [8]. At $\mathrm{Pe}=10^4$, our active two-stage and three-stage mixers give $T_{L2}=0.63$ and $T_{L3}=0.53$, respectively. At a slightly higher Pe (2×10^4), Ref. [8] reports $T_{L2}=0.95$ and $T_{L3}=0.90$; even at a much lower Pe=2000, Ref. [8] reports mixing parameters that correspond to poorer mixing ($T_{L2}=0.74$ and $T_{L3}=0.61$) than we find. It should be noted that in Ref. [8] more complete mixing than presented here was reported with a mixing parameter of $T=0.1$, however, this was achieved after a much longer mixing length $L=10$ mm. In closing, we note that the presented active micromixer performance can be tuned, independent of the flow rate, by selecting the operational parameters of the mixer; the mixer contains no dead volume, streams may be kept separated by opening all valves, and with optimization complete mixing ($T=0$) can be achieved as well.

This research was supported by the Eastman Kodak Company.

[1] N.-T. Nguyen and S. T. Wereley, *Fundamentals and Applications of Microfluidics* (Artech House, Boston, 2006).
[2] J. M. Ottino, *The Kinematics of Mixing* (Cambridge University Press, Cambridge, 1989).
[3] H. Aref, *Chaos Applied to Fluid Mixing* (Pergamon Press, New York, 1995).
[4] J. M. Ottino and S. Wiggins, Science **305**, 485 (2004).
[5] F. G. Bessoth, A. J. deMello, and A. Manz, Anal. Commun. **36**, 213 (1999).
[6] S. W. Lee, D. S. Kim, S. S. Lee, and T. H. Kwon, J. Micromech. Microeng. **16**, 1067 (2006).
[7] T. J. Johnson, D. Ross, and L. E. Locascio, Anal. Chem. **74**, 45 (2002).
[8] A. D. Stroock *et al.*, Science **295**, 647 (2002).
[9] A. O. El Moctar, N. Aubry, and J. Batton, Lab Chip **3**, 273 (2003).
[10] S. Qian, J. Zhu, and H. H. Bau, Phys. Fluids **14**, 3584 (2002).
[11] M. H. Oddy, J. G. Santiago, and J. C. Mikkelsen, Anal. Chem. **73**, 5822 (2001); A. Dodge, A. Hountondji, M. C. Jullien, and P. Tabeling, Phys. Rev. E **72**, 056312 (2005).
[12] H. Song, J. D. Tice, and R. F. Ismagilov, Angew. Chem., Int. Ed. **42**, 767 (2003); P. Garstecki, M. A. Fischbach, and G. M. Whitesides, Appl. Phys. Lett. **86**, 244108 (2005); A. Günther *et al.*, Langmuir **21**, 1547 (2005).
[13] B. Stoeber, C.-M. J. Hu, D. Liepmann, and S. J. Muller, Phys. Fluids **18**, 053103 (2006).
[14] B. Stoeber, Z. Yang, D. Liepmann, and S. J. Muller, J. Microelectromech. Syst. **14**, 207 (2005).
[15] See EPAPS Document No. E-PLEEE8-75-172705 for movies showing mixer operation, the downstream region of the two-stage mixer, and the third mixer stage. For more information on EPAPS, see http://www.aip.org/pubservs/epaps.html.